A study of hadronic shower development in the ECAL of the alpha magnetic spectrometer Ⅱ *

ZANG Jing-Jing(藏京京)[1;1)] CHEN Guo-Ming(陈国明)[1] BIAN Jian-Guo(卞建国)[1]
FAN Jia-Wei(范嘉伟)[1] LI Zu-Hao(李祖豪)[1] LIANG Song(梁松)[1]
MENG Xiang-Wei(孟祥伟)[1] TAO Jun-Quan(陶军全)[1] TANG Zhi-Cheng(唐志成)[1]
WANG Jian(王健)[1] WANG Jian(王健)[2] WANG Xian-You(汪先友)[3]
WANG Zheng(王征)[1] XU Ming(徐明)[1] XU Wei-Wei(许伟伟)[1]
XIAO Hong(肖虹)[1] YAN Qi(严琪)[1] YANG Min(杨民)[1]

[1] Institute of High Energy Physics, Chinese Academy of Sciences, Beijing 100049, China
[2] Graduate University of Chinese Academy of Sciences, Beijing 100049, China
[3] Theoretical Physics Institute, Chongqing University, Chongqing 400044, China

Abstract: In this paper, we studied the development of hadronic shower in an electromagnetic calorimeter of Alpha Magnetic Spectrometer Ⅱ. Two parametrized empirical formulae were proposed to describe the hadronic shower shape in calorimeter. Using 100 GeV proton beam incident on the center of the ECAL, detailed plots of lateral and longitudinal hadronic shower behavior were given and we found the formulae can describe the development of the hadronic shower with the test beam data. The possible application of the parametrized formulae including $e^{\pm}$-$\pi^{\pm}$ discrimination and tau jet reconstruction was discussed.

Key words: hadronic shower, ECAL, parametrisation, $e^{\pm}$-$\pi^{\pm}$ discrimination

PACS: 21.30.Fe, 29.25.Ni, 29.40.Vj **DOI:** 10.1088/1674-1137/35/8/012

1 Introduction

The Alpha Magnetic Spectrometer Ⅱ is a particle physics experiment device designed to mount on the International Space Station (ISS) and detect anti-matter and dark matter by measuring the cosmic ray. The subdetector-Electromagnetic Calorimeter (ECAL) is a sampling calorimeter with a fine grained lead-scintillating fiber structure, which provides a good energy and angular resolution and high e/p discrimination.

With the fine granularity structure, the ECAL has the ability to precisely reconstruct the shower development of particles. Using this property, we studied the average longitudinal and lateral profile of the hadronic shower and developed two empirical formulae to describe the energy distribution of the hadronic shower.

The analysis was organized as follows. Section 2 mainly introduces the structure of the ECAL detector. In Section 3, the beam test setup in the year of 2007 and the strategy of event selections were presented briefly. Two empirical formulae were developed in section 4 to describe the averaged longitudinal and lateral shower shape. Section 5 shortly discusses possible applications. Finally, a conclusion is given in Section 6.

2 The electromagnetic calorimeter structure

The active part of the ECAL called Pancake is composed of nine superlayers (18 layers) for an active area of 64.8 cm×64.8 cm and a thickness of 16.65 cm corresponding to $17X_0$ or $1\lambda_{\rm i}$, where X_0 is the radiation length and $\lambda_{\rm i}$ is the nuclear interaction length

Received 5 November 2010, Revised 10 February 2011

* Supported by National Natural Science Foundation of China (10435070, 10721140381, 10099630), China Ministry of Science and Technology (2007CB16101) and Chinese Academy of Sciences (KJCX2-N17, 1730911111)

1) E-mail: zangjj@ihep.ac.cn

(Fig. 1(a)). Each superlayer is 1.85 cm in thickness and it is made of 11 grooved, 1 cm thick lead foil layers of 0.1 cm in diameter scintillating fibers, glued together with epoxy resin (Fig. 1(b) Fig. 1(c)). The main geometry parameters are shown in Fig. 1(c). In order to measure the three dimensional shower shape, the fiber orientation is rotated by 90° for each ten fiber layers (one superlayer). The schematic diagram of fiber orientation in three superlayers is shown in Fig. 1(d). There are five superlayers with fibers aligned along the magnetic bending direction (y-axis) and four superlayers with fibers aligned along the other direction (x-axis).

The signal lights produced in the scintillating fibers are read out by four-anode Hamamatsu photomultipliers (PMT). Each PMT has an active area of 1.8 cm×1.8 cm subdivided into 2×2 valid cells, therefore, each cell covers 0.9 cm×0.9 cm×64.8 cm in volume which corresponds to 35 fibers. To avoid blind zones brought by the margin of the PMTs, fibers are read only at one end and 36 PMTs are alternately covered at both sides of each superlayer, so one superlayer is separated by PMTs into 2 readout layers, 144 readout cells in total. The Fig. 1(a) shows the PMT positions for each superlayer. More detailed information of the ECAL has been published in Refs. [1, 2].

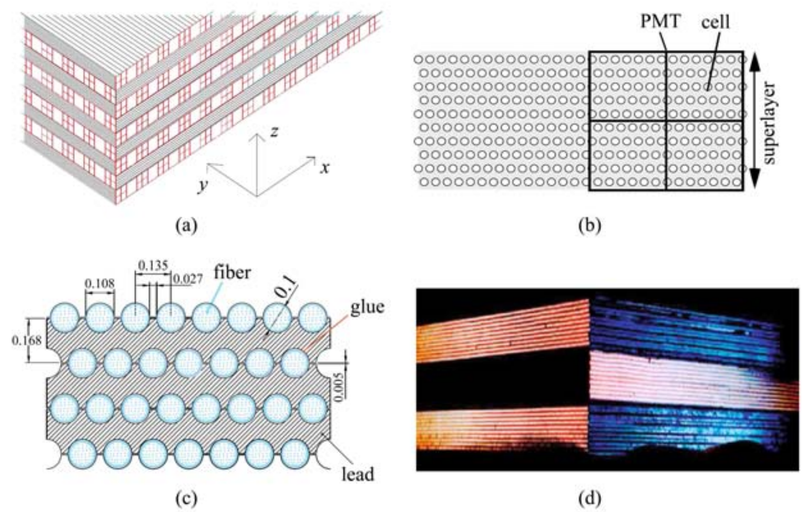

Fig. 1. (a) Schematic view of the ECAL pancake structure, the windows mark the position of each PMT; (b) detailed digram of one superlayer; (c) geometry parameters of lead foil and fiber; (d) fiber orientation in three superlayers.

3 Experimental data and data selection

3.1 Beam test setup

In July 2007, the flight model of the ECAL was successfully tested and calibrated on the H4 beam line of the Super Proton Synchrotron (SPS) at CERN. The schematic plot of the beam test setup is shown in Fig. 2. The whole model is mounted on a rotating table that can move along x and y axes and can rotate around the z axis and this device allows a scanning along the x and y direction. To flag the electron events, particles were identified by two Cherenkov counters at first. Due to very low identification efficiency, those two counters were removed in the end. The event trigger was provided by four crossed scintillator counters. Three ladders of the tracker detector were installed in the front of the ECAL, which can reject multi-particles events and can help to reconstruct beam incident position.

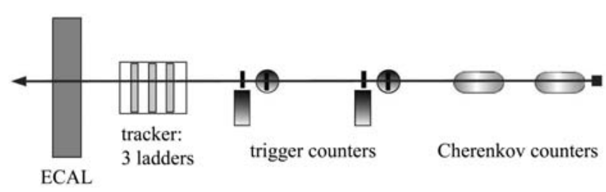

Fig. 2. The ECAL beam test 07 setups.

The proton beam with energy 100 GeV and the electron beam with energy between 6 GeV and 250 GeV were used. To avoid lateral energy leakage, the data samples with 100 GeV proton beam incident on the center of the calorimeter were selected in this paper, shown in Fig. 3. A more detailed introduction to the setup and results of beam test were described in Ref. [2].

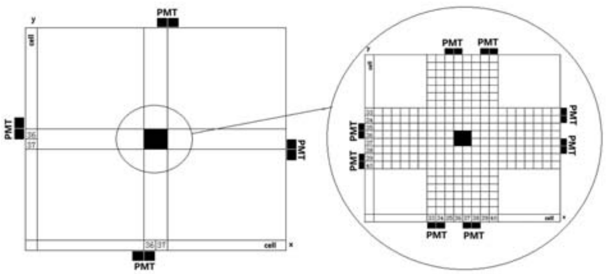

Fig. 3. Schematic view of the test beam setup.

3.2 Data selection

The high-energy proton beams produced by the H4 Beam Line of the SPS usually contains a little fraction (less than 10%) of electrons or muons. In order to reduce this contamination to a reasonable level, we can make use of the fact that hadronic shower spreads wider than electromagnetic shower. The distribution of electron energy is more concentrated in the ECAL with a certain number of hits. This phenomenon is illustrated in Fig. 4, which shows a scatter plot of ADC count (corresponding to the total energy deposited in the ECAL) against the total number of hits. A clear cluster of electrons is visible in the figure. The electrons could be excluded by requiring the ADC count over the total hits less than 32. Although this selection could remove most electron events, it can't reject the rare electron events distributed in transitional region as shown in Fig. 4. Considering most electron showers will take place in two radiation lengths, we required that the starting point of the shower shouldn't be at the first two layers (The starting point will be discussed in Section 4.1). With those two selections the electron contamination is negligible.

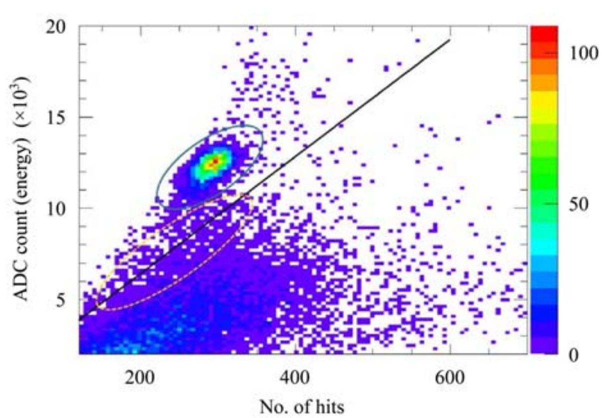

Fig. 4. The scatter plot of ADC count against the total number of hits. Most electron events distribute in the solid circle region. The rare ones locate in the transitional region (the dashed circle region). Events below the black solid line are selected.

During the high energy range, muon events are easily identified due to the small total energy they deposited. Those events would be removed effectively by requiring that particles from beam line generate at least 2000ADC energy and this selection will reject most MIP(minimum ionizing particle) events simultaneously.

4 Parametrization of hadronic shower

4.1 Longitudinal shower

As introduced in Section 2, the whole ECAL is only one nuclear interaction length thick, the hadronic shower may start at any layer of the ECAL. To suppress the fluctuation of the shower caused by the starting point, we developed three simple cuts by summing up the experience to decide the starting point event by event. About 1000 random hadron shower events were selected to manually test the reliability of the cuts, which revealed that more than 90% of the results of the cuts are consistent with the results of the visual scan (using the naked eye to locate the starting point event by event). These three cuts were concluded as follows:

1. The energy deposited in the first shower layer should be less than 100 ADC counts.

2. The energy of one layer should be less than the energy in the next layer and the energy in the next layer should be less than the energy in the next-to-next layer at the same time.

3. The fraction of the sum energy from the first layer to the n-th layer over the sum energy from the n+1 th layer to the n+4 th layer should be less than 0.3.

In Fig. 5, we compare the starting point from the three cuts with the one extracted by visual scan, which shows reasonable agreement. In addition, the chi-square goodness-of-fit statitical tests are performed on the data corresponding to Fig. 5 to further check the consistency between them. As a result of low statistics of the last two bins, we consider them as a single bin in the procdure of the tests. So the χ^2 statistic

$$\chi^2=\sum\nolimits_{i=2}^{12}\frac{\left(n^i_{\rm cuts}-n^i_{\rm hand}\right)^2}{n^i_{\rm hand}}$$

follows the $\chi^2\,(11)$ distribution, where $n^i_{\rm cuts}$ and $n^i_{\rm hands}$ stand for the number of events in the i-th bin extracted by cuts or visual scan separately. In general, the critical value of chi-square $\chi^2_{\alpha=0.05}=19.68$ if the α is chosen to be 0.05. On the other hand, the calculated value of χ^2 for the two histograms in Fig. 5

is 14.27<19.68, which indicates that there is no reason to deny the consistency between the result of cuts and visual scan with the significance level $\alpha=0.05$.

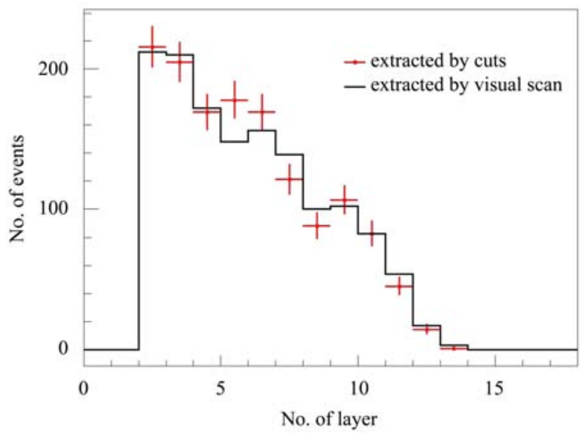

Fig. 5. The starting point of the hadronic shower. The solid line is extracted manually event by event (1400 events in total), dots with statistic error are from the three cuts, which is normalized to 1400 events. The first two layers are removed, in order to reject the electron events.

The mean longitudinal energy profile has been well described by the superposition of two gamma distributions in Ref. [3]. We found that one gamma distribution is enough, if the starting point is known. So the longitudinal hadronic shower shape is described by the function:

$$\frac{\mathrm{d}E}{\mathrm{d}t}=E_0 b\frac{(bt)^{a-1}\,\mathrm{e}^{-bt}}{\Gamma(a)}, \tag{1}$$

where t is a variable standing for the depth from shower starting point. E_0, a and b are free parameters needed to be determined by fitting data. Parameter E_0 corresponds to the impact energy, a and b are dependent on the atomic number Z of the absorber and impact particle energy.

A χ^2 minimization fit is performed to tune the parameters using the MINUIT minimization package. The χ^2 is given by

$$\chi^2=\sum_{\text{layer=stp}}^{18}\left(E_{\text{layer}}^{\text{fitted}}-E_{\text{layer}}^{\text{deposited}}\right)^2, \tag{2}$$

where "stp" is an abbreviation for the starting point, $E_{\text{layer}}^{\text{fitted}}$ and $E_{\text{layer}}^{\text{deposited}}$ denote the energy calculated by Formula 1 in one layer and deposited in that layer separately. In the calculation of $E_{\text{layer}}^{\text{fitted}}$, the Simpson integration is used to integrate the function through the corresponding layer.

Figure 6 exhibits the average longitudinal profile of 100 GeV proton showers, separately for the measuring results (the solid line) and the fitting results (the dots with error bar). The mean value of the energy deposited in each layer is determined by averaging the number of ADC counts for all events. In the same way, the result of fits to Formula 1 is calculated by averaging the fitted energy for all events. As we expect, the deposited energies in all layer are consistent with the fitting results. In addition, the distributions of parameters a and b are shown in Fig. 7, they are all in the reasonable region.

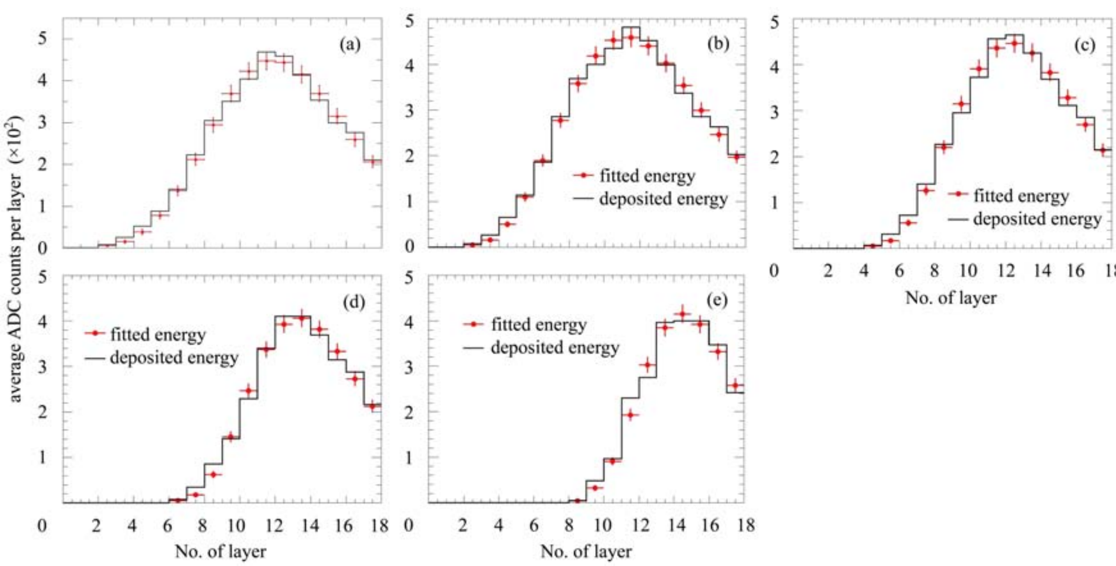

Fig. 6. The longitudinal shower profile of 100 GeV proton, the solid line represents the mean value of the deposit energy in each layer, the dots with error bars are the average energy expected from Formula 1 in each layer. Only statistic error is considered in the plot. (a) The total longitudinal shower profile; (b) The starting point at the 2nd layer; (c) The starting point at the 4th layer; (d) The starting point at the 6th layer; (e) The starting point at the 8th layer.

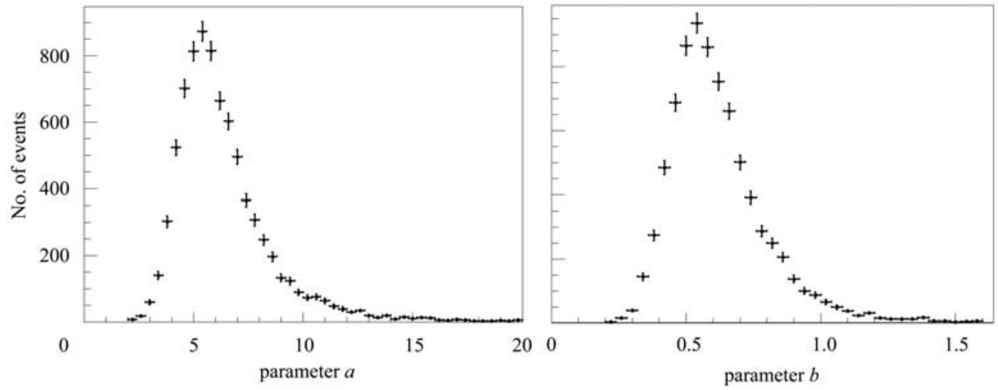

Fig. 7. The distributions of parameters a and b.

4.2 Lateral shower

For the description of the lateral profile shower shape, we developed an empirical formula,

$$\frac{\mathrm{d}^2 E}{\mathrm{d}x\mathrm{d}y}=\frac{E_{\mathrm{t}}}{2\pi}\frac{\Gamma(B)}{\Gamma(B-2)}\frac{R^{B-2}}{(r+R)^B},$$
$$r=\sqrt{(x-x_{\mathrm{c}})^2+(y-y_{\mathrm{c}})^2}, \tag{3}$$

where r is a variable representing the distance from the shower central gravity; E_{t}, R, B, x_{c} and y_{c} are free parameters obtained by fitting data with Formula 3. E_{t} stands for the total incident energy; x_{c} and y_{c} represent the shower's center of gravity and are in unit of cell; R and B are free parameters to determine the shower shape. Considering that the hadronic shower shape is axial symmetry, there is only one COG (center of gravity) parameter left, when the shower shape is projected to x or y axis. Other analytic formulae including superposition of two exponentials (Ref. [4]) or combination of one Gaussian and one exponential (Ref. [5]) are tried. However, Formula 3 is the simplest one which has only four free parameters with the similar agreement between the fitted result and the beam test data sample. In order to compare the beam test data with the empirical formula, a χ^2 minimization is performed similarly with Section 4.1, where the χ^2 is given by

$$\chi^2=\sum_{\mathrm{cell}=0}^{72}\left(E_{\mathrm{cell}}^{\mathrm{fitted}}-E_{\mathrm{cell}}^{\mathrm{deposited}}\right)^2, \tag{4}$$

where $E_{\mathrm{cell}}^{\mathrm{deposited}}$ is the deposited energy summing over the same cells at each layer, the $E_{\mathrm{cell}}^{\mathrm{fitted}}$ is calculated by the integration over the same region as $E_{\mathrm{cell}}^{\mathrm{deposited}}$. Fig. 8 shows the proton shower transverse profiles extracted from the beam test data sample and the parametrized formula. As we expect, the fitted energy agrees well with the deposited energy in three orders in the central region. However, for the range far away from the shower axis, they have a little discrepancy which is caused by edge effect.

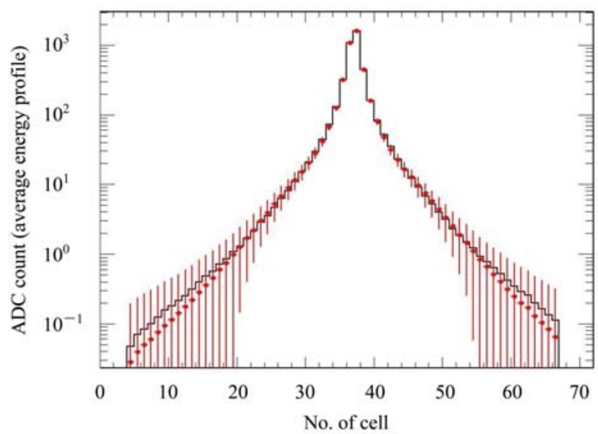

Fig. 8. The average lateral energy profile as a function of number of cell. The curve is the average lateral profile of deposited energy. The dots with error bars are the fitted result using Formula 3. Only statistic error is shown.

5 Discussion about the possible applications

In the particle physics experiment, $e^{\pm}$-$\pi^{\pm}$ can be distinguished easily at low energy through several kinds of detectors, such as the time of flight detector, transition radiation detector or different $\mathrm{d}E/\mathrm{d}x$ in tracker detector. During the high energy range, the electron (or positron) has a very similar behavior with charged pion in these three detectors, which makes it difficult to discriminate them. However, $e^{\pm}$-$\pi^{\pm}$ discrimination can be achieved by making use of the different starting points of the shower in calorimeter between electron and charged pion. In addition, the distribution of the electron shower is more concentrated than the charged pion shower. So, if we use

Formula 3 to fit the lateral shower shapes, parameters and χ^2 will differ greatly for the electron and charged pion.

In the Higgs search with the channel H$\rightarrow \tau\tau$ at a very high energy, in a collider experiment like the LHC, the τ with high energy can cascade decay to $\pi^{\pm}$, π^0 and ν_τ ($\tau^{\pm} \rightarrow \rho^{\pm}\pi^0\nu_\tau \rightarrow \pi^{\pm}\pi^0\pi^0\nu_\tau$). The $\pi^{\pm}$ and π^0 will be boosted heavily by the energy of tau, which makes them too close to identify. The shower generated by $\pi^{\pm}$ and π^0 will overlap in the calorimeter and will be detected as a single cluster. Using Formula 3, the single cluster can be separated into the hadronic part and the electromagnetic part. Then the position and energy of π^0 and $\pi^{\pm}$ can be obtained to reconstruct the invariant mass of ρ. This will suppress the background efficiently for the Higgs search.

6 Conclusion

In this paper, we investgated the lateral and longitudinal energy profile of hadronic shower with data sample obtained from the ECAL beam test. For the description of the longitudinal hadronic shower profile, we found that one Γ-distribution is enough after comparing with two or more Γ-distributions, if the starting point of the shower has been known. On the other hand, an empirical formula was developed to describe the average lateral profile of hadronic showers. We have also compared the average deposited energy in the ECAL with the expected result from our formula and found that there is general agreement between them in three orders. Finally, two possible applications were discussed.

References

1 Cadoux F et al. Nuclear Physics B (Proc. Suppl.), 2002, **113**(1-3): 159–165

2 Falco Stefano. Advances in Space Research, 2010, **45**(1): 112–122

3 Grindhammer G et al. Nuclear Instruments and Methods in Physics Research Section A: Accelerators, Spectrometers, Detectors and Associated Equipment, 1990, **290**(2-3): 469–488

4 Archurin N et al. Nuclear Instruments and Methods Physics Research Section A: Accelerators, Spectrometers, Detectors and Associated Equipment, 1997, **399**(2-3): 202–226

5 Amaral P et al. Nuclear Instruments and Methods Physics Research Section A: Accelerators, Spectrometers, Detectors and Associated Equipment, 2000, **443**(1): 51–70